Environ. Sci. Technol. **2010,** *44,* 9488–9495

C_{60} Aminofullerene Immobilized on Silica as a Visible-Light-Activated Photocatalyst

JAESANG LEE,[†,‡] YURI MACKEYEV,[§] MIN CHO,[∥] LON J. WILSON,[§] JAE-HONG KIM,[∥] AND PEDRO J. J. ALVAREZ*,[†]

Department of Civil and Environmental Engineering, Rice University, Houston, Texas 77005, United States, Water Environment Center, Korea Institute of Science and Technology, Seoul 136-791, Korea, Department of Chemistry and the Smalley Institute for Nanoscale Science and Technology, Rice University, Houston, Texas 77005, United States, and Department of Civil and Environmental Engineering, Georgia Institute of Technology, Atlanta, Georgia 30332, United States

Received August 18, 2010. Revised manuscript received October 19, 2010. Accepted October 27, 2010.

A new strategy is described to immobilize photoactive C_{60} aminofullerene on silica gel (3-(2-succinic anhydride)propyl functionalized silica), thus enabling facile separation of the photocatalyst for recycling and repeated use. An organic linker moiety containing an amide group was used to anchor C_{60} aminofullerene to the functionalized silica support. The linker moiety prevents aqueous C_{60} aggregation/agglomeration (shown by TEM images), resulting in a remarkable enhancement of photochemical $^1O_2$ production under visible light irradiation. With no loss in efficacy of $^1O_2$ production plus insignificant chemical modification of the aminoC_{60}/silica photocatalyst after multiple cycling, the system offers a promising new visible-light-activated photocatalyst. Under visible-light irradiation, the aminoC_{60}/silica photocatalyst is capable of effective and kinetically enhanced oxidation of Ranitidine and Cimetidine (pharmaceutical pollutants) and inactivation of MS-2 bacteriophage compared to aqueous solutions of the C_{60} aminofullerene alone. Thus, this photocatalyst could enable water treatment in less developed areas by alleviating dependence on major infrastructure, including the need for electricity.

Introduction

Providing access to safe water is an overriding global challenge that is rapidly growing as the world's population increases, as rising sea levels threaten saline intrusion, and as municipal and industrial wastes continue to pollute water supplies. This pressing challenge is stimulating technological innovation for water treatment, including photocatalytic and advanced oxidation processes (*1, 2*). Such emerging technologies might enable a water recycling and distributed treatment paradigm to alleviate dependence on major system infrastructure (critical for rural areas and expanding large cities in developing countries), avoid health risks associated with harmful disinfection byproducts formed during chlorination or ozonation of drinking water (*3, 4*), exploit alternative water sources, and abate energy consumption and water quality degradation associated with aging water distribution systems.

The unique photochemical properties of C_{60} enable equimolar photon conversion to singlet oxygen ($^1O_2$) upon irradiation with photon energy exceeding 2.3 eV (< 550 nm) (*5, 6*). Such a high yield of $^1O_2$ generation offers a promising application for C_{60} and its derivatives as a proxy for photodynamic therapeutic reagents (*7*−*9*) or as a synthetic catalyst (*10*) for Diels−Alder and Ene reactions. In addition, another practical use of C_{60} and its derivatives as a novel environmental photocatalyst was recently described using visible light (or sunlight)-assisted $^1O_2$ production (*5, 6*) and the oxidizing capacity of $^1O_2$ for pollutant degradation (*11*−*13*) and microbial inactivation (*13*−*17*).

Our earlier findings demonstrated that water-soluble C_{60} derivatives displayed a high efficacy for photochemical $^1O_2$ production and associated bacterial/viral inactivation (*13*). C_{60} aminofullerene (with quaternary ammonium nitrogen atoms) was particularly effective for virus inactivation under visible and sunlight irradiation (*13, 15*). However, aqueous dissolution of C_{60} with hydrophilic functional groups represents challenges for recycling the photocatalyst (as well as concerns about unintended environmental release) which impacts its cost-effective and eco-responsible use. These concerns suggest the need for immobilization of the photocatalyst.

$^1O_2$ photosensitizer dyes such as Rose Bengal have been previously immobilized on silica to achieve photodynamic inactivation of bacteria (*18*) and on polymers for photooxygenation in aqueous media (*19*). Jensen et al. (*10*) and Hino et al. (*20*) also attached pristine-C_{60} to amine-functionalized silica and polymer beads to facilitate separation of C_{60}-based agents during heterogeneous photosynthesis. However, immobilization of derivatized C_{60} (including aminofullerenes, with demonstrated aqueous availability and antimicrobial activity (*13*)) and relevant photocatalytic activity has not been previously addressed in the literature. To our knowledge, the immobilization of functionalized C_{60} for the purpose of environmental cleanup has not been attempted either.

In order to facilitate C_{60} application in water treatment and disinfection, we herein propose covalent-bond immobilization of C_{60} aminofullerene to surface-functionalized silica gel. We synthesized water-soluble C_{60} aminofullerenes and their immobilized forms (aminoC_{60}/silica) and evaluated their comparative kinetics for photochemical $^1O_2$ production. In addition, the use of aminoC_{60}/silica as a viable environmental photocatalyst is assessed in terms of 1) $^1O_2$ generation kinetics under visible-light illumination, 2) catalytic use and relevant chemical stability, and 3) photocatalytic oxidation of pharmaceuticals and photodynamic viral inactivation.

Experimental Section

Preparation of C_{60} Aminofullerenes. Chemicals for the synthesis (Table S1) were used without purification. Malonic acid bis-(2-*tert*-butoxycarbonylamino-ethyl) ester was prepared as described elsewhere (*15*). The C_{60} aminofullerene derivatives were synthesized as carbamates according to established procedure (*13*), with the synthetic conditions summarized in Table S2. The adducts were isolated using liquid chromatography and converted to hydrochloric acid

* Corresponding author phone: (713)348-5903; fax: (713)348-5203; e-mail: alvarez@rice.edu.

[†] Department of Civil and Environmental Engineering, Rice University.

[‡] Water Environment Center, Korea Institute of Science and Technology.

[§] Department of Chemistry and the Smalley Institute for Nanoscale Science and Technology, Rice University.

[∥] Department of Civil and Environmental Engineering, Georgia Institute of Technology.

10.1021/es1028475

© 2010 American Chemical Society

Published on Web 11/15/2010

SCHEME 1. Strategy for Immobilization of Water-Soluble C_{60} Aminofullerenes on the Functionalized Silica Gel (n = 2, 4, and 6)

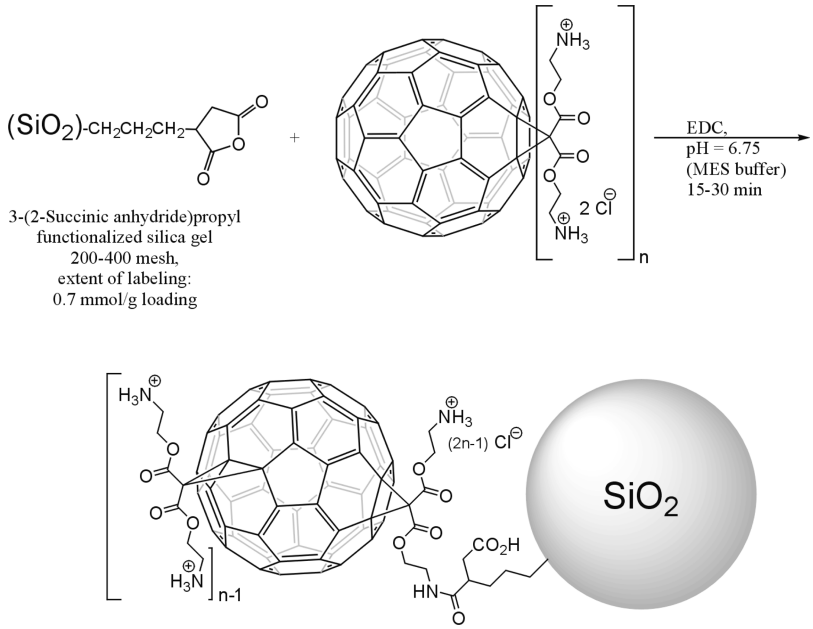

salts using 6 M HCl solution in a water-dioxane mixture (1:2.5) for 4 h at 30 °C. The final C_{60} aminofullerenes were purified with a cellulose ester dialysis membrane (Spectra/Por, MWCO = 500D) for 14 days using DI water (adjusted to pH ≈ 4 by adding 0.1 mL of concentrated HCl solution to 1 L of water) and freeze-dried in vacuum.

Immobilization of C_{60} Aminofullerenes on Silica Gel. The C_{60} aminofullerenes were immobilized on silica gel using a novel approach illustrated in Scheme 1, with the synthetic conditions summarized in Table S3. The water-soluble condensing reagent, N-(dimethylaminopropyl)-N′-ethylcarbodiimide hydrochloride, was used in the presence of catalytic amounts of 1-hydroxybenzotriazol hydrate, to form an amide bond between C_{60} aminofullerene derivatives and 3-(2-succinic anhydride)propyl functionalized silica gel (extent of labeling: 0.7 mmol/g loading; particle size: 200−400 mesh; surface area: 500 m^2/g, Sigma Aldrich). The optimal coupling conditions were achieved at room temperature in aqueous solution buffered at pH = 6.75 with 10% 2-(N-morpholino)ethanesulfonic acid (MES) sodium salt. C_{60} aminofullerene-coated silica (aminoC_{60}/silica) was separated from solution using 0.2-μm nylon filters (Nylaflo, Pall Corp.), further washed with distilled water and acetonitrile, and dried in vacuum. The amount of C_{60} aminofullerene loaded on silica was determined using an SDT 2960 Universal V3.4C TA thermogravimetric analyzer/differential scanning calorimeter (TGA/DSC). Covalent bond formation between silica and the aminofullerenes was verified using a Nexus 670 Thermo-Nicolet FTIR spectrometer in the range of 500−4000 cm^{-1} with a Golden Gate diamond crystal attenuated total reflectance (ATR) device. Morphological features of the aminoC_{60}/silica material were determined after drying on a carbon grid using a JEM 100C transmission electron microscope (TEM) (Jeol, Peabody, MA) with 100 kV electron beam.

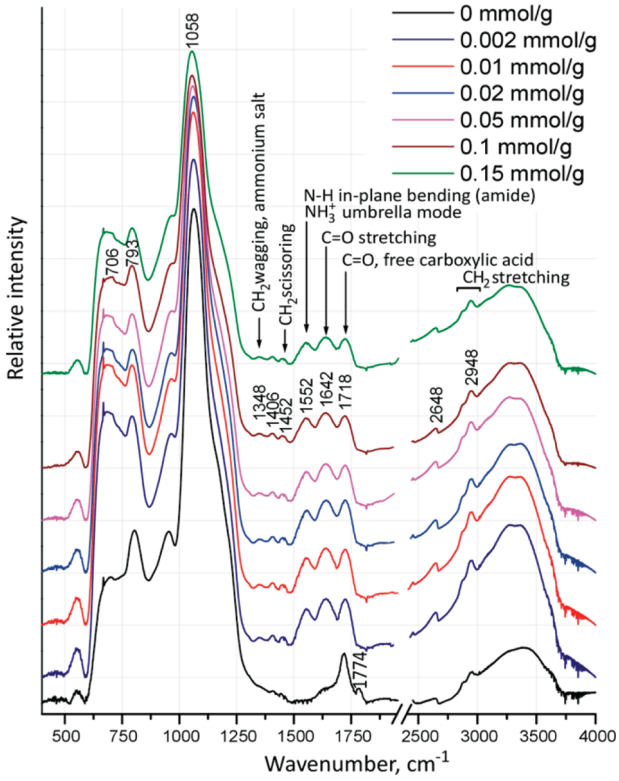

FIGURE 1. FT-IR spectra of hexakis-aminoC_{60}/silica. The dominant peak around 1060 cm^{-1} corresponds to Si−O−Si asymmetric stretching mode. Peaks at 1348, 1552, 1642 cm^{-1} are present in FT-IR spectra only when hexakis-C_{60} aminofullerene is chemically bound to silica gel.

Photochemical $^1O_2$ Production and Pollutant Degradation. Testing of the water-soluble C_{60} aminofullerenes (or their immobilized forms) for photochemical $^1O_2$ generation and pollutants degradation was performed in aqueous solutions (or suspensions) (10 mM phosphate buffer at pH 7.0) using a magnetically stirred 60 mL cylindrical quartz reactor surrounded by six 4-W commercial fluorescence lamps (emission wavelength: 350−650 nm (*15*), Philips Co.) at ambient temperature (22 °C). All experiments were carried out in air-equilibrated aerobic conditions. The light intensity of fluorescent lamp at a representative wavelength of 365 nm was measured as 165 μW/cm^2 using a UVX radiometer with 365 longwave sensor (UVP Co., Upland, CA, USA) placed at the same position as the quartz reactor. Experiments to examine visible light activation of C_{60} aminofullerenes (homogenized and immobilized) were carried out with a UV cutoff filter which blocks irradiation of UV fractions in lamp emission spectrum (< 400 nm). Reaction suspensions con-

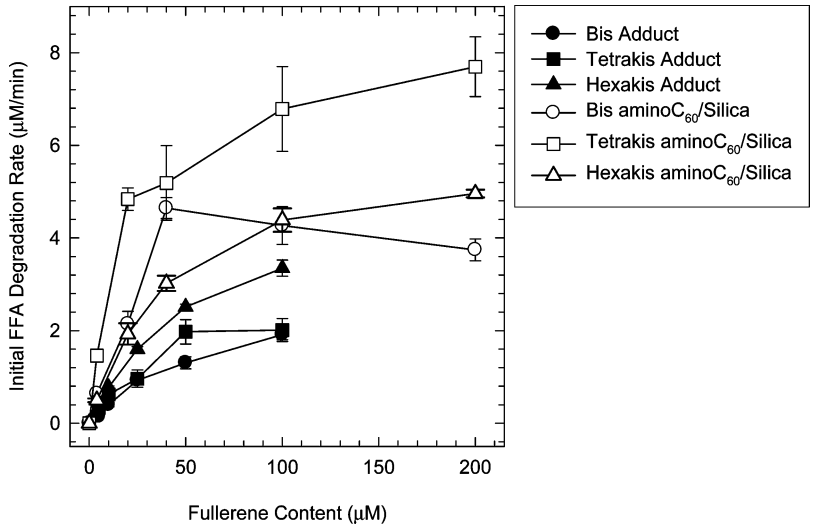

FIGURE 2. Initial rates (20 min) for photochemical FFA degradation; i.e., photosensitized $^1O_2$ production, by bis-, tetrakis-, and hexakis-C_{60} aminofullerenes suspended in water and immobilized on silica as a function of fullerene content ([aminoC_{60}/silica]$_0$ = 2 g/L (× 0.002 mmol/*g* = 4 μM; × 0.01 mmol/*g* = 20 μM; × 0.02 mmol/*g* = 40 μM; × 0.05 mmol/*g* = 100 μM; × 0.01 mmol/*g* = 200 μM); [FFA]$_0$ = 0.25 mM; [phosphate]$_0$ = 10 mM; pH$_i$ = 7).

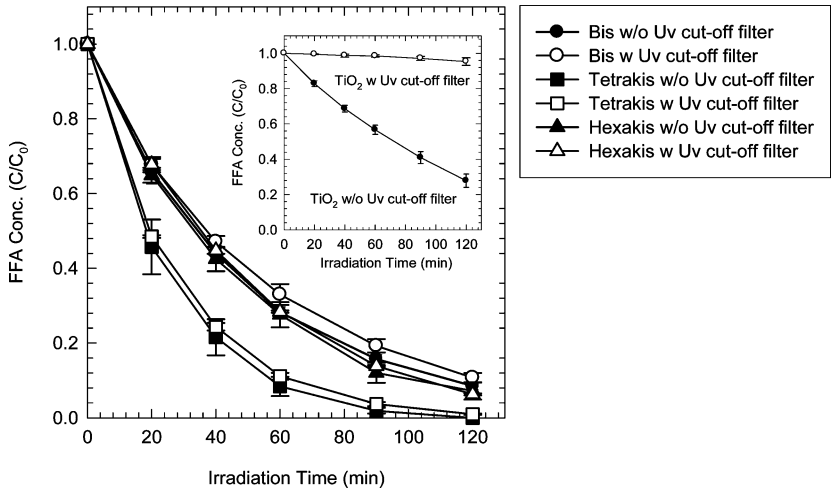

FIGURE 3. FFA degradation by bis-, tetrakis-, and hexakis-aminoC$_{60}$/silica with a fullerene content of 0.05 mmol/g under visible-light irradiated conditions and under commercial fluorescence lamp irradiation. Inset: FFA degradation by TiO_2 photocatalyst under visible light and under commercial fluorescence lamp irradiation ([aminoC$_{60}$/silica]$_0$ = 2 g/L; [TiO_2]$_0$ = 2 g/L; [FFA]$_0$ = 0.25 mM; [phosphate]$_0$ = 10 mM; pH$_i$ = 7).

taining C_{60} aminofullerenes (homogenized and immobilized) at desired concentrations and 0.25 mM furfuryl alcohol (FFA) (as an indicator for $^1O_2$ (*13, 21, 22*)) or 0.1 mM target contaminant (e.g., Ranitidine and Cimetidine) were buffered at pH 7 using 10 mM phosphate. During the course of the photochemical reaction, sample aliquots of 1 mL were withdrawn from the reactor using a syringe, filtered through a 0.22-μm PTFE filter (Millipore), and injected into a 2-mL amber glass vial for further analysis. The residual FFA (or Ranitidine and Cimetidine) concentration at a constant time interval was monitored using a HPLC (Waters 2695) equipped with a C-18 column (Nova-Pak C18) and a photodiode-array detector (Waters 996).

Antibacterial Activity. The antibacterial property of the aminofullerenes was assessed under dark and anaerobic conditions (thus eliminating the potential for production of reactive oxygen species) to evaluate the potential intrinsic (acute) toxicity of the inactivated photocatalyst. This was quantified by measuring the minimum inhibitory concentration (MIC). Briefly, *E. coli* (ATCC DH5α) cultured overnight in Luria−Bertani broth was spiked into modified Minimal Davis medium (*23*) containing varying concentrations of the aminofullerenes. Growth of *E. coli* was monitored as optical density (absorbance) at 600 nm (OD_{600}) using an Agilent 8453 UV−vis spectrophotometer. The minimum concentration of the aminofullerenes which resulted in no growth of *E. coli* after 18 h of incubation was denoted as the MIC.

Photoinduced Viral Inactivation. The experimental suspension (10 mM phosphate buffer at pH 7.0) contained either 30 μM of soluble C_{60} aminofullerene suspended in water or immobilized on silica and 2×10^5 plaque forming unit (pfu)/mL MS-2 bacteriophage (ATCC 15597). The suspension was placed in a 40 mL quartz reactor and irradiated at ambient temperature (22 °C) with a 4-W fluorescence lamp, and a 1 mL sample aliquot was collected at different times. Viability of MS-2 phage was quantified by the soft agar overlay, plaque assay method using *E. coli* (C3000) at exponential to early stationary phase as the host. Phage stock was prepared using the same *E. coli* as the host via confluent lysis.

Results and Discussion

$^1O_2$ Production by Aqueous C_{60} Aminofullerene Solutions. Bis-, tetrakis-, and hexakis-adducts of C_{60} amino-

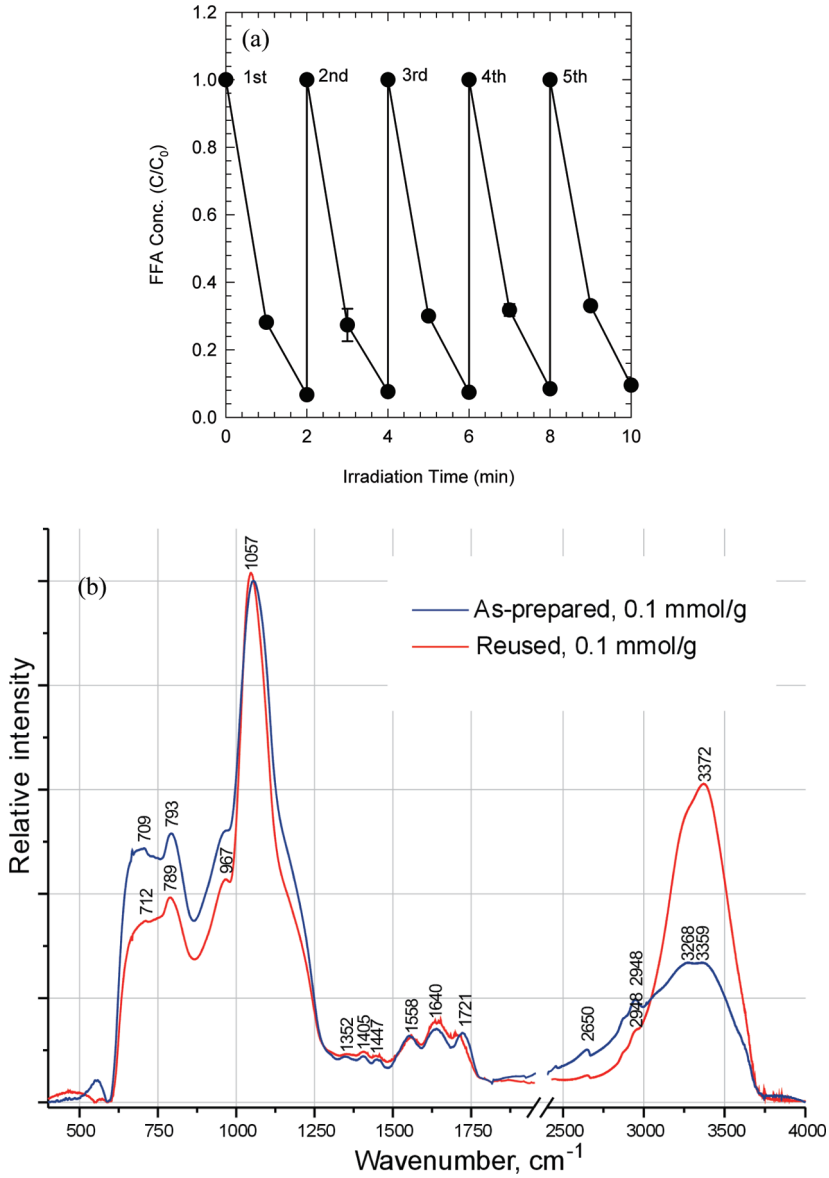

FIGURE 4. (a) Repeated degradation of FFA by hexakis-aminoC_{60}/silica with a fullerene content of 0.05 mmol/g under visible light illumination and (b) FT IR for the freshly prepared hexakis-aminoC_{60}/silica (blue line) vs a five time reused sample (red) ([hexakis-aminoC_{60}/silica]$_0$ = 2 g/L; [FFA]$_0$ = 0.25 mM; [phosphate]$_0$ = 10 mM; pH$_i$ = 7).

fullerenes (Table S4) effectively photocatalyzed the degradation of FFA, which served as surrogate for $^1O_2$ generation under fluorescent light illumination (Figure S1, Supporting Information). Negligible FFA decay occurred either with white light alone or in the presence of the C_{60} aminofullerenes under dark conditions (data not shown). Addition of L-histidine as a $^1O_2$ scavenger (*13, 15, 22*) at an excess concentration (50 mM) caused drastic retardation in FFA decomposition, while excess *t*-BuOH as a $^{\bullet}$OH scavenger (*22, 24*) negligibly affected the FFA degradation kinetics. This corroborates that FFA decay is attributed to photochemical production of $^1O_2$ by the C_{60} aminofullerenes in aqueous solutions.

Immobilization of C_{60} Aminofullerene on Silica Gel. Peaks at 1552 and 1642 cm^{-1}, which are assigned to N−H and C=O of amide bond, appeared in the FT-IR spectra of the bis-, tetrakis-, and hexakis-adducts of C_{60} aminofullerene-derivatized silica materials (bis-, tetrakis-, and hexakis-aminoC_{60}/silica), as shown in Figure 1 for hexakis-aminoC_{60}/silica, and in Figures S2 and S3 for bis- and tetrakis-aminoC_{60}/silica materials, respectively. These IR peaks were not present for the underivatized 3-(2-succinic anhydride)propyl functionalized silica gel. A weak IR signal, located at 1774 cm^{-1} in the underivatized silica gel which can be assigned to the asymmetric vibration of the succinic anhydride ring, disappeared in the course of derivatization with aminofullerenes. This same IR peak pattern was identically observed in the FT-IR spectra of bis- through hexakis-aminoC_{60}/silica materials (Figures 1, S2 and S3). This observation implies chemical linkage of the amine-terminated groups of the aminofullerene to the carboxylic acid moiety of the functionalized silica gel via amide bond formation. The increase in aminofullerene content on silica leads to a color change of the hexakis-aminoC_{60}/silica material from yellow to dark purple (Figure S4a). In the UV−vis reflectance spectra of hexakis-aminoC_{60}/silica (Figure S4b), the absorbance in the visible light wavelength region grows proportionally to the amounts of aminofullerenes immobilized.

Immobilization Improves Photochemical $^1O_2$ Production. Figure 2 compares the initial rates of photochemical $^1O_2$ generation by homogenized and immobilized forms of the aminofullerenes as a function of fullerene content. Although localization of the aminofullerenes on silica gel likely may offer much less access to incident photons and

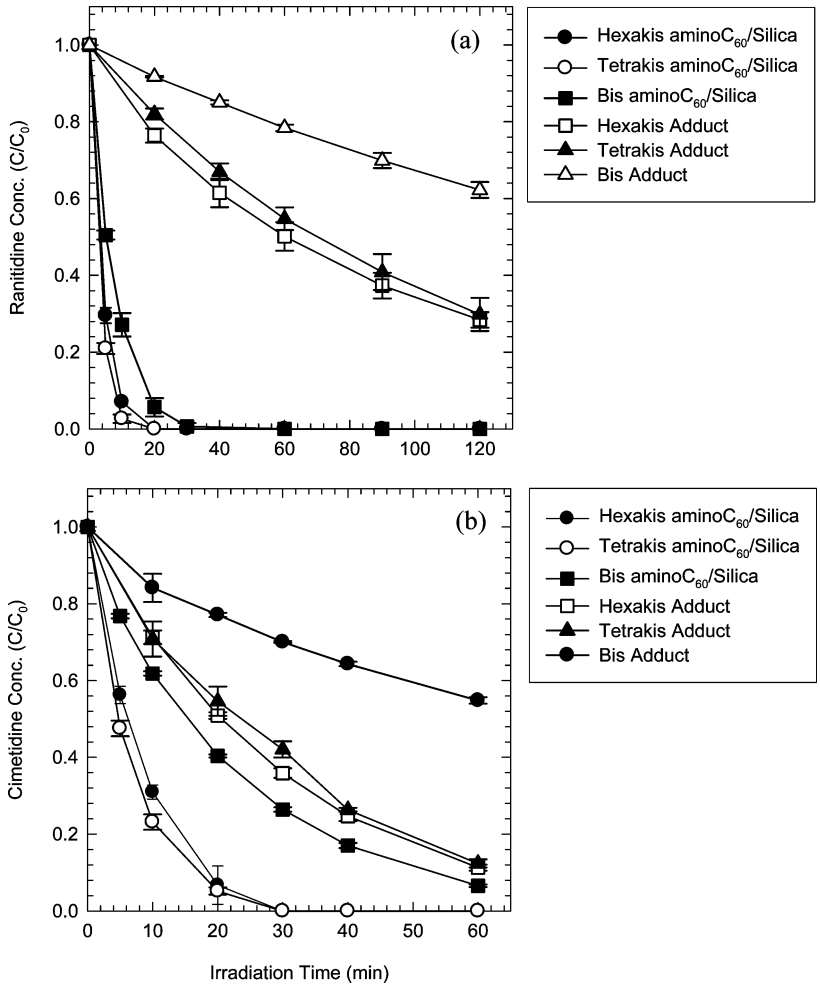

FIGURE 5. Degradation of (a) Ranitidine and (b) Cimetidine by bis-, tetrakis-, and hexakis-C_{60} aminofullerenes and bis-, tetrakis-, and hexakis-aminoC_{60}/silica with a fullerene content of 0.1 mmol/g under visible light irradiated conditions. ([C_{60} aminofullerene] = 100 μM; [aminoC_{60}/silica]$_0$ = 1 g/L; [Ranitidine]$_0$ = [Cimetidine]$_0$ = 0.1 mM; [phosphate]$_0$ = 10 mM; pH$_i$ = 7).

FFA, the bis-, tetrakis-, and hexakis-aminoC_{60}/silica materials all achieved more rapid $^1O_2$ production than the homogenized forms dissolved in aqueous solutions based on initial FFA degradation rates. The bare functionalized silica gel was not photoactive for $^1O_2$ generation, and no FFA adsorption on the silica occurred. Immobilized bis- and tetrakis-adducts of C_{60} aminofullerene displayed substantially enhanced efficacy in $^1O_2$ production, which was about 2 to 4 times higher than in aqueous suspensions of their homogenized forms. The kinetic comparison suggested that bis- and tetrakis-aminoC_{60}/silica materials photochemically produced $^1O_2$ at a comparable or higher rate than hexakis-aminoC_{60}/silica, while the rate of $^1O_2$ generation by aminofullerene solutions was in the order of hexakis- > tetrakis- > bis-.

It is highly likely that the improved photoactivity of C_{60} aminofullerenes loaded on silica is attributed to decreased C_{60} aggregation/agglomeration. Our earlier finding (*13*) showed that in aqueous phosphate solution, the hexakis-adduct of aminofullerene formed aggregates (several hundred nanometers to the micrometer size) that retain photoactivity. This is different than the water-stable C_{60} clusters (nC_{60}), which experience significantly diminished $^1O_2$ production efficacy (if any), possibly due to a self-quenching/triplet−triplet annihilation (*22, 25*) and likely shrinkage of the active surface area. Such aggregation and associated loss of photoreactivity are likely precluded to some extent as the C_{60} aminofullerenes are immobilized on silica. TEM analysis (Figure S5b) shows little aggregation/agglomeration of the hexakis-adduct of C_{60} aminofullerene on the silica surface, compared to the much larger amorphous aggregates of the C_{60} aminofullerenes suspended in water (Figure S5c). The TEM image of unmodified silica gel control does not show the aminofullerene deposits on the silica surface (Figure S5a).

Visible-Light-Induced $^1O_2$ Production. As expected from visible light (λ > 400 nm)-induced $^1O_2$ production by homogenized forms (Figure S6), aminoC_{60}/silica enables effective FFA degradation, i.e. $^1O_2$ generation, with visible light (Figure 3). No significant difference in $^1O_2$ production rate was observed between with and without UV cutoff filter. On the other hand, under the identical visible-light irradiation, TiO_2 photocatalyst (Degussa P25) known to be activated only with UV light (λ < 380 nm) (*1*) barely induced FFA degradation, while rapidly oxidized FFA in the absence of UV cutoff filter (inset of Figure 3).

Catalytic Performance for $^1O_2$ Generation. FFA degradation by hexakis-adduct of aminoC_{60}/silica was repeated over five cycles under visible-light irradiation. FFA oxidation in each cycle was performed in different batches using aminoC_{60}/silica, which was separated after photoreaction through cellulose filter paper with a pore size of 25 μm (allowing penetration of homogenized form) and washed 4 times with 100 mL of Milli-Q water. As shown in Figure 4a, photoactivity of hexakis-aminoC_{60}/silica for $^1O_2$ production was negligibly reduced over the multiple cycles. Release of aminofullerenes after each cycle was not measurable by UV−vis spectroscopy on the permeate solutions. Insignificant loss of fullerene content from silica was verified by comparison of TGA plots for freshly prepared and reused hexakis-aminoC_{60}/silica (five

TABLE 1. Minimal Inhibitory Concentration (MIC) Values of a Series of Water-Soluble C_{60} Aminofullerenes[a]

aminofullerene adducts	aminofullerene solution concentration (μM)						
	0	40	80	120	160	200	400
bis-adduct	+	+	+	+	+	+	+
tetrakis-adduct	+	+	+	+	−	−	−
hexakis-adduct	+	+	+	+	−	−	−

[a] +, positive microbial growth; −, no growth.

times) (data not shown). FT-IR spectrum for the freshly prepared hexakis-aminoC_{60}/silica (blue line) vs a reused sample (red) showed insignificant spectral changes, indicating no loss of amide bond between hexakis-adduct and the functionalized silica (Figure 4b). C=O stretching, attributed to the carbonyl band of the free carboxylic acid, shifted from 1721 to 1706 due to pH adjustment (salt formation).

Photoinduced Pharmaceutical Contaminants Degradation. Ranitidine and Cimetidine, which are pharmaceuticals and personal care products (PPCPs) considered as emerging contaminants (*26, 27*), were rapidly degraded by bis-, tetrakis-, and hexakis-adducts of aminoC_{60}/silica materials under visible light illuminated conditions (Figure 5). The kinetic comparison showed that immobilization on silica resulted in significant acceleration in degradation rates of both pharmaceuticals, which is compatible with the aforementioned enhancement in $^1O_2$ generation. The improvement in photochemical degradation kinetics of Ranitidine and its fast adsorption on silica under dark condition (Figure S7) indicates that the silica support possibly functions as an adsorbent to offer a better chance for singlet oxygenation of pollutant substrates on the surface of the aminoC_{60}/silica. However, considering that singlet oxygen rarely achieves mineralization of organic pollutants, further studies are recommended to determine the distribution and potential toxicity of intermediates formed by photosensitized singlet oxygenation.

Potential Acute Toxicity of Inactivated Photocatalyst. The antibacterial activity of the inactivated aminofullerenes (under dark and anaerobic conditions) was used as an indicator of potential intrinsic (acute) toxicity. Results shown in Table 1 suggest that the MIC of tetrakis- and hexakis-adducts of C_{60} aminofullerene to *E. coli* was 120 to 160 μM, whereas bis-adduct of C_{60} aminofullerene did not exhibit antibacterial property up to 400 μM. As previously discussed (*13*), these intrinsic antibacterial properties might be related to the positively charged amino functional groups on the C_{60} aminofullerenes which closely interact with negatively charged *E. coli*, although the detailed mechanism is unknown. Accordingly, fewer amino groups in the bis-adduct of C_{60} aminofullerene might have contributed to decreased antibacterial property of this material compared to the tetrakis- and hexakis-adducts. Overall, the relatively high MIC values compared to common priority pollutants (*28*) suggest low potential intrinsic acute toxicity of the inactivated photocatalyst.

Photoinduced Virus Inactivation. Figure 6 shows the results of MS-2 phage inactivation by aminofullerenes under fluorescence lamp irradiation. Similar to our previous work (*15*), a control test confirmed that MS-2 phage was not inactivated without light or aminofullerenes. In general, MS-2 phage inactivation was faster when the

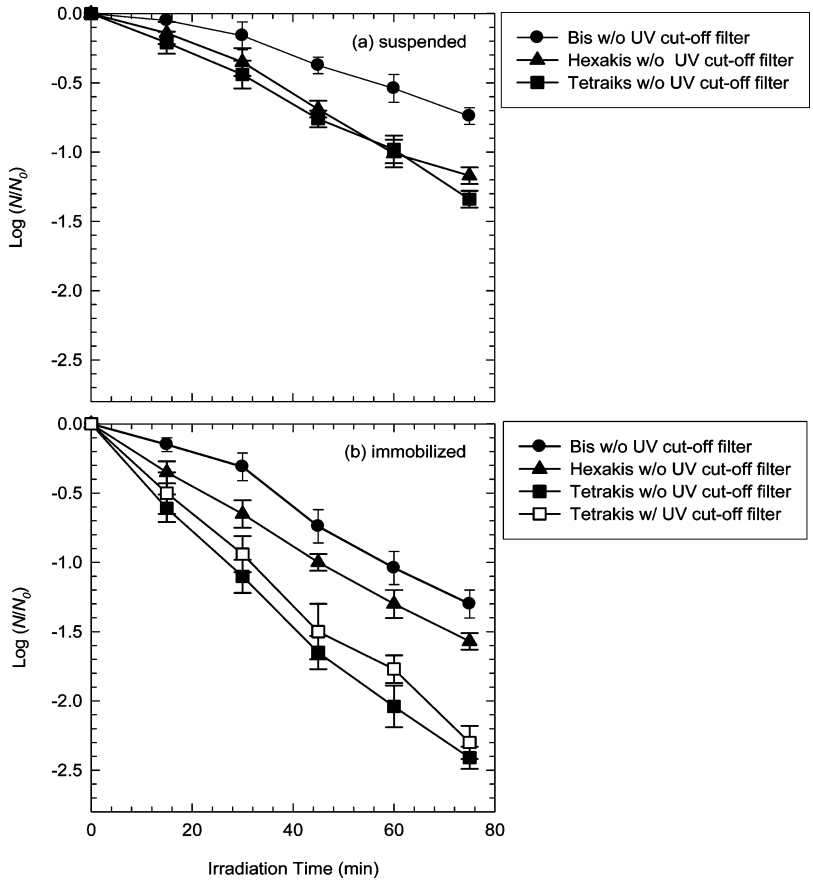

FIGURE 6. MS-2 phage inactivation by (a) suspended bis-, tetrakis-, and hexakis-C_{60} aminofullerenes and (b) immobilized bis-, tetrakis-, and hexakis-aminoC_{60}/silica with a fullerene content of 0.05 mmol/g under visible light and under commercial fluorescence lamp irradiation (22 °C; [C_{60} aminofullerene]$_0$ = 15 μM; [aminoC_{60}/silica]$_0$ = 0.3 g/L; [MS-2]$_0$ = 2 × 10^5 pfu/mL; [phosphate]$_0$ = 10 mM; pH$_i$ = 7). *N* is the number of viable MS-2 phage remaining, and N_0 is the initial number.

aminofullerenes were immobilized (Figure 6). The immobilized tetrakis-adduct of aminofullerene also exhibited higher $^1O_2$ production efficacy than the water-soluble counterpart at the same molar concentration (indicated by nearly twice as fast FFA removal rates (Figure S8)). In addition, MS-2 phage inactivation was completely inhibited by 30 mM L-histidine (data not shown), suggesting that $^1O_2$ is the primary agent for phage inactivation. Consequently, the inactivation kinetics correlated well with the FFA degradation kinetics (Figure S8). Note that inactivation kinetics were only slightly changed when a UV filter was used to cutoff lights below 400 nm, implying that $^1O_2$ production and subsequent MS-2 phage inactivation by the aminofullerenes photocatalysis were primarily induced by visible-light.

As the range and scope of pollution in water systems continue to increase, novel high performance systems are needed to fill the gaps where conventional water treatment is unavailable, marginally effective, or not feasible. This work enhanced the potential use of C_{60} as a visible-light-activated environmental photocatalyst by chemically immobilizing C_{60} aminofullerenes on functionalized silica gel. In addition to enabling facile separation, immobilization of C_{60} aminofullerenes on silica support accelerated photochemical $^1O_2$ production and increased the efficiency of pollutants degradation and viral inactivation. Such enhanced photoreactivity of aminoC_{60}/silica is possibly due to prevention of C_{60} clustering on silica, which may increase reactive surface area and retard self-quenching mechanism and triplet−triplet annihilation. Further tests with various types of recalcitrant pollutants and more resistant microorganisms under "real world" conditions (e.g., presence of natural organic matter) are needed to assess the feasibility and transformative technological potential of aminoC_{60}/silica, although the demonstrated degradation of Ranitidine and Cimetidine and photodynamic MS-2 inactivation with visible light illumination are encouraging.

Acknowledgments

This work was funded by the National Science Foundation (Award #: CBET-0932872). Partial funding was also provided by the Center for Biological and Environmental Nanotechnology (NSF Award EEC-0647452) and by the Robert A. Welch Foundation (Grant C-0627).

Supporting Information Available

Synthesis recipe and conditions for C_{60} aminofullerenes (homogenized and immobilized forms) and chemical structures of C_{60} aminofullerenes and rates for $^1O_2$ production by homogenized C_{60} aminofullerenes under fluorescence lamp and visible light irradiations. Ranitidine and Cimetidine adsorption tests as well as additional characterization data such as FT-IR spectra of bis- and tetrakis-aminoC_{60}/silica, UV−visible diffuse reflectance spectra of a series of hexakis-aminoC_{60}/silica, and TEM images of bare silica, hexakis-aminoC_{60}/silica, and homogenized hexakis-adduct. This material is available free of charge via the Internet at http://pubs.acs.org.

Literature Cited

(1) Hoffmann, M. R.; Martin, S. T.; Choi, W. Y.; Bahnemann, D. W. Environmental applications of semiconductor photocatalysis. *Chem. Rev.* **1995**, *95*, 69–96.
(2) Kamat, P. V.; Meisel, D. Nanoscience opportunities in environmental remediation. *C. R. Chim.* **2003**, *6*, 999–1007.
(3) Pinkernell, U.; von Gunten, U. Bromate minimization during ozonation: Mechanistic considerations. *Environ. Sci. Technol.* **2001**, *35*, 2525–2531.
(4) Zhang, X. R.; Minear, R. A.; Barrett, S. E. Characterization of high molecular weight disinfection byproducts from chlorination of humic substances with/without coagulation pretreatment using UF-SEC-ESl-MS/MS. *Environ. Sci. Technol.* **2005**, *39*, 963–972.
(5) Arbogast, J. W.; Darmanyan, A. P.; Foote, C. S.; Rubin, Y.; Diederich, F. N.; Alvarez, M. M.; Anz, S. J.; Whetten, R. L. Photophysical properties of C_{60}. *J. Phys. Chem.* **1991**, *95*, 11–12.
(6) Lof, R. W.; van Veenendaal, M. A.; Koopmans, B.; Jonkman, H. T.; Sawatzky, G. A. Band gap, excitons, and coulomb interaction in solid C_{60}. *Phys. Rev. Lett.* **1992**, *68*, 3924–3927.
(7) Ikeda, A.; Doi, Y.; Nishiguchi, K.; Kitamura, K.; Hashizume, M.; Kikuchi, J. I.; Yogo, K.; Ogawa, T.; Takeya, T. Induction of cell death by photodynamic therapy with water-soluble lipid-membrane-incorporated [60]fullerene. *Org. Biomol. Chem.* **2007**, *5*, 1158–1160.
(8) Iwamoto, Y.; Yamakoshi, Y. A highly water-soluble C_{60}-NVP copolymer: A potential material for photodynamic therapy. *Chem. Commun.* **2006**, 4805–4807.
(9) Wang, S. Z.; Gao, R. M.; Zhou, F. M.; Selke, M. Nanomaterials and singlet oxygen photosensitizers: Potential applications in photodynamic therapy. *J. Mater. Chem.* **2004**, *14*, 487–493.
(10) Jensen, A. W.; Daniels, C. Fullerene-coated beads as reusable catalysts. *J. Org. Chem.* **2003**, *68*, 207–210.
(11) Chae, S. R.; Hotze, E. M.; Wiesner, M. R. Evaluation of the oxidation of organic compounds by aqueous suspensions of photosensitized hydroxylated-C_{60} fullerene aggregates. *Environ. Sci. Technol.* **2009**, *43*, 6208–6213.
(12) Han, S. K.; Bilski, P.; Karriker, B.; Sik, R. H.; Chignell, C. F. Oxidation of flame retardant tetrabromobisphenol A by singlet oxygen. *Environ. Sci. Technol.* **2008**, *42*, 166–172.
(13) Lee, J.; Mackeyev, Y.; Cho, M.; Li, D.; Kim, J.-H.; Wilson, L. J.; Alvarez, P. J. J. Photochemical and antimicrobial properties of novel C_{60} derivatives in aqueous systems. *Environ. Sci. Technol.* **2009**, *43*, 6604–6610.
(14) Badireddy, A. R.; Hotze, E. M.; Chellam, S.; Alvarez, P.; Wiesner, M. R. Inactivation of bacteriophage via photosensitization of fullerol nanoparticles. *Environ. Sci. Technol.* **2007**, *41*, 6627–6632.
(15) Cho, M.; Lee, J.; Mackeyev, Y.; Wilson, L. J.; Alvarez, P. J. J.; Hughes, J. B.; Kim, J. H. Visible light sensitized inactivation of MS-2 bacteriophage by a cationic amine-functionalized C_{60} derivative. *Environ. Sci. Technol.* **2010**, *44*, 6685–6691.
(16) Schafer, M.; Schmitz, C.; Facius, R.; Horneck, G.; Milow, B.; Funken, K. H.; Ortner, J. Systematic study of parameters influencing the action of Rose Bengal with visible light on bacterial cells: Comparison between the biological effect and singlet-oxygen production. *Photochem. Photobiol.* **2000**, *71*, 514–523.
(17) Spesia, M. B.; Milanesio, A. E.; Durantini, E. N. Synthesis, properties and photodynamic inactivation of Escherichia coli by novel cationic fullerene C_{60} derivatives. *Eur. J. Med. Chem.* **2008**, *43*, 853–861.
(18) Guo, Y. Y.; Rogelj, S.; Zhang, P. Rose Bengal-decorated silica nanoparticles as photosensitizers for inactivation of gram-positive bacteria. *Nanotechnology* **2010**, *21*, 1–7.
(19) Schaap, A. P.; Thayer, A. L.; Zaklika, K. A.; Valenti, P. C. Photooxygenations in aqueous solution with a hydrophilic polymer-immobilized photosensitizer. *J. Am. Chem. Soc.* **1979**, *101*, 4016–4017.
(20) Hino, T.; Anzai, T.; Kuramoto, N. Visible-light induced solvent-free photooxygenations of organic substrates by using [60]fullerene-linked silica gels as heterogeneous catalysts and as solid-phase reaction fields. *Tetrahedron Lett.* **2006**, *47*, 1429–1432.
(21) Haag, W. R.; Hoigne, J. Singlet oxygen in surface waters. 3. Photochemical formation and steady-state concentrations in various types of waters. *Environ. Sci. Technol.* **1986**, *20*, 341–348.
(22) Lee, J.; Fortner, J. D.; Hughes, J. B.; Kim, J. H. Photochemical production of reactive oxygen species by C_{60} in the aqueous phase during UV irradiation. *Environ. Sci. Technol.* **2007**, *41*, 2529–2535.
(23) Cho, M.; Fortner, J. D.; Hughes, J. B.; Kim, J. H. Escherichia coli inactivation by water-soluble, ozonated C_{60} derivative: Kinetics and mechanisms. *Environ. Sci. Technol.* **2009**, *43*, 7410–7415.
(24) Vonpiechowski, M.; Thelen, M. A.; Hoigne, J.; Buhler, R. E. Tert-butanol as an OH radical scavenger in the pulse radiolysis of oxygenated aqueous systems. *Ber. Bunsen-Ges. Phys. Chem.* **1992**, *96*, 1448–1454.
(25) Lee, J.; Yamakoshi, Y.; Hughes, J. B.; Kim, J. H. Mechanism of C_{60} photoreactivity in water: Fate of triplet state and radical anion and production of reactive oxygen species. *Environ. Sci. Technol.* **2008**, *42*, 3459–3464.

(26) Anderson, P. D.; D'Aco, V. J.; Shanahan, P.; Chapra, S. C.; Buzby, M. E.; Cunningham, V. L.; Duplessie, B. M.; Hayes, E. P.; Mastrocco, F. J.; Parke, N. J.; Rader, J. C.; Samuelian, J. H.; Schwab, B. W. Screening analysis of human pharmaceutical compounds in US surface waters. *Environ. Sci. Technol.* **2004**, *38*, 838–849.
(27) Latch, D. E.; Stender, B. L.; Packer, J. L.; Arnold, W. A.; McNeill, K. Photochemical fate of pharmaceuticals in the environment: Cimetidine and Ranitidine. *Environ. Sci. Technol.* **2003**, *37*, 3342–3350.
(28) Wu, C. C.; Shryock, T. R.; Lin, T. L.; Fleck, M. Testing antimicrobial susceptibility against Mycoplasma hyopneumoniae in vitro. *Swine Health Prod.* **1997**, *5*, 227–230.

ES1028475